

---

# Know Your Limits: Monotonicity & Softmax Make Neural Classifiers Overconfident on OOD Data

---

Dennis Ulmer\*  
 IT University Copenhagen  
 dennis.ulmer@mailbox.org

Giovanni Cinà\*  
 Pacmed BV  
 giovanni.cina@pacmed.nl

## Abstract

A crucial requirement for reliable deployment of deep learning models for safety-critical applications is the ability to identify out-of-distribution (OOD) data points, samples which differ from the training data and on which a model might underperform. Previous work has attempted to tackle this problem using uncertainty estimation techniques. However, there is empirical evidence that a large family of these techniques do not detect OOD reliably in classification tasks.

This paper puts forward a theoretical explanation for said experimental findings. We prove that such techniques are not able to reliably identify OOD samples in a classification setting, provided the models satisfy weak assumptions about the monotonicity of feature values and resulting class probabilities. This result stems from the interplay between the saturating nature of activation functions like sigmoid or softmax, coupled with the most widely-used uncertainty metrics.

## 1 Introduction

Notwithstanding the tremendous improvements achieved in recent years by means of novel and larger deep learning architectures, advanced models still lack certain properties that guarantee their safety in high-stakes applications like health care [17], autonomous driving [38], and more. Among other traits, the capability to discern familiar data samples seen during the training stage (in-distribution) from abnormal inputs (out-of-distribution) is paramount in certain contexts. Take for instance a hospital, in which an algorithm is used to predict complications for a patient. Due to factors like changing patient demographics or protocols but also simply different hospital environments, predictions might become less reliable and cause harm to the patient. A degradation of the model performance might only be detected much later, when the shift in the test data becomes more apparent - at which point further damage accumulates. Whence the need arises to implement techniques that can detect OOD samples reliably.

Unfortunately, it is well-known that neural network classifiers tend to be overconfident in their predictions [15], i.e. exhibiting high levels of certainty when it is unwarranted, and often fail to correctly identify OOD samples [41]. A recent study on medical tabular data has shown that even techniques specifically developed to quantify the model's uncertainty struggle at detecting OOD samples for a relatively simple classification task [51]. Crucially, it was shown that neural discriminators tend to project vast areas of high certainty far away from the training distribution - a behaviour that seems completely at odds with reliable OOD detection. These observations can easily be replicated on synthetic data, as displayed in Figure 1, where one can observe areas of high certainty represented in white stretching beyond the training data. The reasons for this behavior in a classification setting are hitherto much less studied.

---

\*The authors contributed equally.

In this paper we propose a novel theoretical argument to explain the observed phenomena. Our contributions are as follows:

1. Our first result shows that, under weak assumptions about the monotonicity between features and conditional class probabilities, standard architectures for single neural network classifiers coupled with widely used uncertainty metrics always lead to high certainty on OOD samples.
2. We extend the aforementioned result by proving that ensembling methods and several uncertainty estimation techniques suffer from the same problem, see Theorem 1.

These results entail that, when the conditions of the theorem are met, these models cannot be used to reliably detect OOD. Albeit restricted by the assumptions on monotonicity, the findings of this article have bearings on OOD detection for several critical applications, including predictions of complications in clinical settings and prediction of mortgage default (see the discussion in Section 6).

## 2 Related Work

Overconfidence in neural networks has been studied from several angles; we summarize here some of the main lines of research. One way to counteract the problem of overconfidence lies in the quantification of a network’s uncertainty, which is usually divided into aleatoric and epistemic uncertainty. The former denotes *non-reducible* uncertainty, e.g. uncertainty intrinsic to the data generating process, while the latter refers to *reducible* uncertainty. This includes the knowledge about the best model class, as well as about the optimal parameters which explain the data best [10, 20]. In this article, we are interested in the effect of methods that estimate uncertainty post-hoc. There are recent approaches which try to account for both types in their architecture, using prior [35] and posterior networks [6], these however remain outside the scope of this work. One way to evaluate

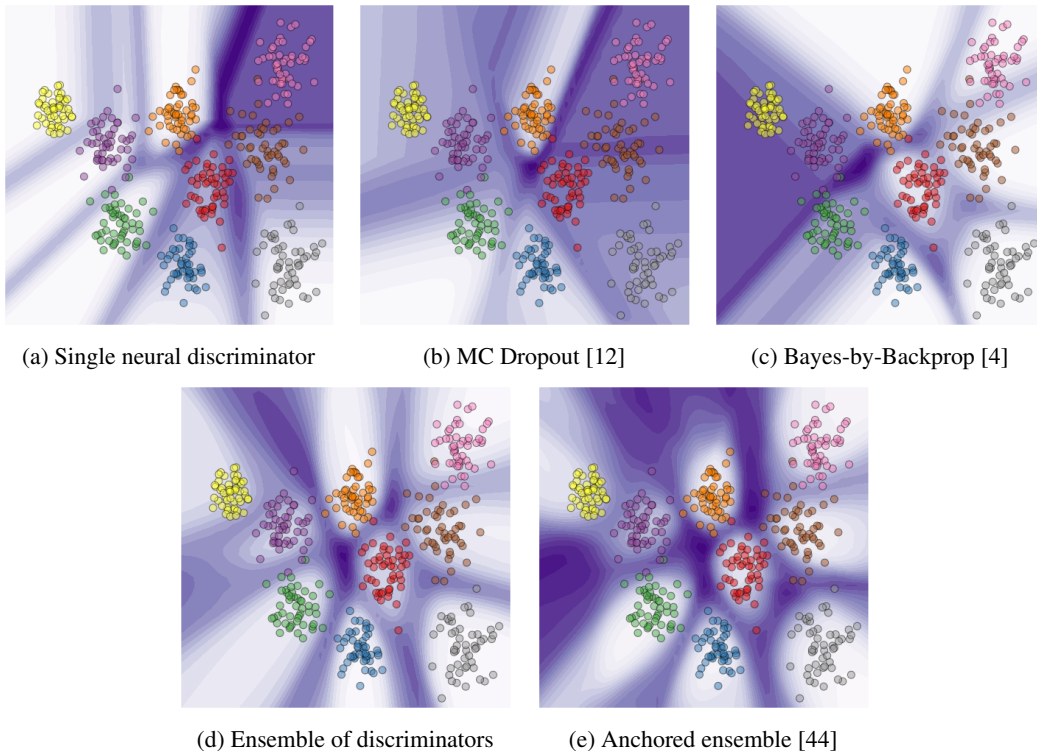


Figure 1: Predictive entropy of different models on a synthetic multi-class classification problem. Predictive entropy, a metric capturing uncertainty, is represented with increasingly darker shades of purple, with white being the lowest uncertainty. Single discriminators (first row) display large open-ended decision regions with low entropy, even where training data is not present. This effect is only partially mitigated by ensemble models (second row).

uncertainty estimation methods is the study of their behaviour in presence of OOD samples [43]. Meijerink et al. [39] and Ulmer et al. [51] specifically show how the methods used in our work fail in practice to detect clinically relevant OOD groups of patients in a medical context. Kompa et al. [26] conclude that many uncertainty methods produce confidence intervals which do not include the actual observations on OOD data.

A variety of articles approached the phenomenon of overconfidence from a calibration perspective: starting with the work of Guo et al. [15], follow-up work developed improved variants of temperature scaling [32] or new types of scaling [27, 28] as well as novel training procedures altogether [50]. A separate line of enquiry investigated the effect of different activation functions [45, 5], exploring alternatives to the sigmoid or softmax function<sup>1</sup> as the final component of neural discriminators [9, 30, 37]. Some of them are motivated by the so-called *softmax bottleneck* issue [46, 3], arguing that it hinders the networks representational capacity [53, 23] or leads to premature saturation during training [7]. Kumar et al. [29] motivate their proposed alternative of a continuous embedding output layer by the computational disadvantages that occur when the number of classes is large, like in the field of natural language processing when predicting the next token out of a language’s dictionary. General properties of the softmax function in the context of reinforcement learning were discussed by [13]. Many authors note the relationship between softmax and network overconfidence [1, 18], but to the best of our knowledge none gives a detailed theoretical explanation for this behavior.

### 3 Preliminaries

We first introduce some necessary background information: in Section 3.1 we introduce notation, in Section 3.2 we explain the notions of data set shift, in Section 3.3 we introduce the uncertainty metrics we will study, and in Section 3.4 we provide some additional definitions that will be used in the rest of this work.

#### 3.1 Notation

We denote sets in calligraphic letters, e.g.  $\mathcal{I}$  or  $\mathcal{C}$ . Vectors are denoted using lower-case bold letters such as  $\mathbf{x}$  or  $\theta$ . For simplicity, we distinguish instantiations from their variables by adding a subscript or a superscript, such as  $\mathbf{x}_i$  and  $\mathbf{x}'$ . For some functions with multiple outputs, a lowercase index refers to a specific component of the output, e.g. with a function  $f : \mathbb{R} \rightarrow \mathbb{R}^N$ ,  $f(x)_n$  denotes one of the output components with  $n \in 1, \dots, N$ . Furthermore, we use  $\odot$  to denote the Hadamard product and  $\|\dots\|_2$  for the  $l_2$ -norm.

#### 3.2 Out-of-Distribution Data

The following definitions of a data set are used throughout this work:

**Definition 1.** *Given a set  $\mathcal{C} = \{1, \dots, C\}$  of numbers denoting class labels, a data set is defined as a set  $\mathcal{D} \subset \mathbb{R}^D \times \mathcal{C}$  containing  $N$  ordered pairs of  $D$ -dimensional feature vectors  $\mathbf{x}_i$  and corresponding class labels  $y_i$  obtained from some (unknown) joint distribution  $\mathbf{x}_i, y_i \sim p(\mathbf{x}, y)$  s.t.  $\mathcal{D} = \{(\mathbf{x}_i, y_i)\}_{i=1}^N$ .*

Although there exist many different notions of dataset shift [47, 40], we particularly focus on *covariate shift*, in which the distribution of feature values - the covariates - differs from the original training distribution  $p(\mathbf{x})$ . We focus on this kind of shift as it is especially common in non-stationary environments like healthcare [40], but also prevalent in many other applications such as image classification [49] or autonomous agents [2].

To simulate covariate shift, we obtain OOD samples by shifting points away from the training distribution by means of a scaling factor. This approach is in line with recent experiments on covariate shift and OOD detection [51, 43]. We would expect a reliable OOD detection model to output increasingly higher uncertainty as points stray further and further away from the mass of  $p(\mathbf{x})$ , thus we study the behaviour of OOD detection models in the limit, when the scaling factor is allowed to grow indefinitely in at least one dimension.

---

<sup>1</sup>Their relationship is outlined in more detail in Appendix A.1 or [5].

### 3.3 Uncertainty Metrics

We begin by defining a neural discriminator. In the following we assume the neural discriminator to follow common architectural conventions, i.e. to consist of a series of affine transformations with ReLU activation functions.

**Definition 2.** *A neural discriminator is a function  $p_{\theta} : \mathbb{R}^D \rightarrow [0, 1]^C$  mapping a  $D$ -dimensional input vector to a categorical probability distribution over  $C$  classes. The function is parametrized by a parameter vector denoted with  $\theta$ .*

We also presuppose the common structure of a neural discriminator by parameterizing a categorical distribution using the softmax function [5]:

**Definition 3.** *The unnormalized output of the network after  $L$  layers is a function  $f_{\theta} : \mathbb{R}^D \rightarrow \mathbb{R}^C$  with the final output following after an additional softmax function  $\bar{\sigma}(\cdot)$  s.t.  $p_{\theta}(y = c | \mathbf{x}) \equiv \bar{\sigma}(f_{\theta}(\mathbf{x}))_c$ .*

The softmax function  $\bar{\sigma} : \mathbb{R}^C \rightarrow \mathbb{R}^C$  is commonly defined as follows:

$$\bar{\sigma}(f_{\theta}(\mathbf{x}))_c = \frac{\exp(f_{\theta}(\mathbf{x})_c)}{\sum_{c'=1}^C \exp(f_{\theta}(\mathbf{x})_{c'})} \quad (1)$$

We now proceed to lay out the uncertainty metrics investigated in this article, starting with the baseline for OOD detection introduced by Hendricks and Gimpel [18], which involves reporting the highest probability across all classes:

$$y_{\max} = \max_{c \in \mathcal{C}} p_{\theta}(y = c | \mathbf{x})$$

The underlying intuition is that the model would predict more uniform distributions for samples with higher uncertainty, therefore producing a lower  $y_{\max}$  score. The other uncertainty estimation techniques introduced below try to approximate the uncertainty of the predictive distribution for a new data point  $\mathbf{x}'$ , which is commonly factorized as follows:

$$p(y | \mathbf{x}', \mathcal{D}) = \int p(y | \mathbf{x}', \theta) p(\theta | \mathcal{D}) d\theta$$

In the following, we use  $p(y | \mathbf{x}, \theta) = p_{\theta}(y | \mathbf{x})$ . The factorization of this equation is intractable: the weight posterior  $p(\theta | \mathcal{D})$  cannot be computed precisely because - as the predictive distribution itself - it contains an integral over a continuous parameter space. Hence the weight posterior is often replaced by a variational posterior  $q(\theta)$  and the expectation formed by this expression is commonly approximated by a Monte-Carlo approximation:

$$\mathbb{E}_{p(\theta | \mathcal{D})} \left[ p_{\theta}(y | \mathbf{x}) \right] \approx \frac{1}{K} \sum_{k=1}^K p_{\theta}^{(k)}(y | \mathbf{x})$$

This expression is calculated by retrieving a set of  $K$  predictions, e.g. by sampling a set of weights from the (variational) posterior [4, 44], markov-chain Monte-Carlo procedures [52, 42] or simply ensembling [31]. An array of uncertainty estimation techniques then build on these aggregated predictions. One of the simplest ones is to compute the class variance [22, 24]:

$$\bar{\sigma}^2 = \frac{1}{C} \sum_{c=1}^C \mathbb{E}_{p(\theta | \mathcal{D})} \left[ \left( p_{\theta}(y = c | \mathbf{x}) \right)^2 \right] - \mathbb{E}_{p(\theta | \mathcal{D})} \left[ p_{\theta}(y = c | \mathbf{x}) \right]^2$$

Conceptually, a high variance can be interpreted as a large degree of disagreement or uncertainty between predictions. Another common metric is the predictive entropy [11]:

$$\tilde{\mathbb{H}} \left[ p_{\theta}(y | \mathbf{x}) \right] = \mathbb{H} \left[ \mathbb{E}_{p(\theta | \mathcal{D})} \left[ p_{\theta}(y | \mathbf{x}) \right] \right]$$

where  $\mathbb{H}$  denotes Shannon entropy. As the entropy is computed on the averaged aggregated predictions, the entropy is low when probability mass is distributed uniformly across all classes, implying that not all predictions were able to single out a clear candidate class. Conversely, entropy is high when all classifiers accumulate mass on a single class, showing a low degree of uncertainty about the current sample. Lastly, we also consider mutual information approximated as in [11, 48]:

$$\underbrace{\mathbb{I}(y, \theta | \mathbf{x})}_{\text{Model uncertainty}} \approx \underbrace{\mathbb{H}\left[\mathbb{E}_{p(\theta | \mathcal{D})}\left[p_{\theta}(y | \mathbf{x})\right]\right]}_{\text{Total uncertainty}} - \underbrace{\mathbb{E}_{p(\theta | \mathcal{D})}\left[\mathbb{H}\left[p_{\theta}(y | \mathbf{x})\right]\right]}_{\text{Data uncertainty}}$$

Intuitively, this is supposed to measure the information gain about the ideal model parameters by receiving a label  $y$ . If the possible gain is low, that means that current parameters are close to the optimal ones, demonstrating a low degree of epistemic uncertainty. While other metrics capture both aleatoric and epistemic uncertainty of the model jointly, approximate mutual information is exclusively concerned with the latter.

### 3.4 Additional Definitions

Here we introduce some concepts related to monotonicity, which will become central in the next sections.

**Definition 4.** A function  $f : \mathbb{R} \rightarrow \mathbb{R}$  is called *monotonically increasing* for  $x, y \in \mathbb{R}$  if  $x \leq y \iff f(x) \leq f(y)$  and *strictly increasing* iff  $f(x) < f(y)$ . We call a function *strictly increasing* on an interval  $\mathcal{I} = [a, b]$  with  $a < b$  and  $a, b \in \mathbb{R}$  if it holds that

$$\forall x' \in \mathcal{I} \left( \frac{\partial}{\partial x} f(x) \Big|_{x=x'} > 0 \right)$$

where  $\cdot|_{x=x'}$  refers to evaluating the value of the derivative of  $f$  at  $x'$ . Conversely, we call the opposite inequalities of the two aforementioned cases *monotonically decreasing* and *strictly decreasing* functions, respectively.

**Definition 5.** We call a function *strictly monotonic* on an interval  $\mathcal{I} = [a, b]$  with  $a < b$  with  $a, b \in \mathbb{R}$  if it is exclusively either strictly increasing or strictly decreasing on the interval.

These definitions can also be extended to multivariate functions by requiring strict monotonicity in all dimensions:

**Definition 6.** We call a multivariate function  $f : \mathbb{R}^D \rightarrow \mathbb{R}$  *strictly monotonic* on a  $D$ -interval  $\mathcal{I} = \mathcal{I}_1 \times \dots \times \mathcal{I}_D \subseteq \mathbb{R}^D$  if it holds that

$$\forall d \in 1, \dots, D, \left( \forall \mathbf{x}' \in \mathcal{I}, \left( \nabla_{\mathbf{x}} f(\mathbf{x}) \Big|_{\mathbf{x}=\mathbf{x}'} \right)_d < 0 \vee \forall \mathbf{x}' \in \mathcal{I}, \left( \nabla_{\mathbf{x}} f(\mathbf{x}) \Big|_{\mathbf{x}=\mathbf{x}'} \right)_d > 0 \right) \quad (2)$$

where  $(\cdot)_d$  refers to  $\frac{\partial f(x_d)}{\partial x_d}|_{x_d=x'_d}$ , the  $d$ -th component of the gradient  $\nabla_{\mathbf{x}} f(\mathbf{x})$  evaluated at  $\mathbf{x}'$ . We call a multivariate function  $f : \mathbb{R}^D \rightarrow \mathbb{R}^C$  *component-wise strictly monotonic* if the above definition holds for the gradient of every output component  $\nabla_{\mathbf{x}} f(\mathbf{x})_c$ .

We note here that the softmax is an example for a component-wise strictly increasing and therefore strictly monotonic function.

As later lemmas investigate the behavior of functions in the limit, it is furthermore useful to define intervals that are unbounded in at least one direction:

**Definition 7.** We call an interval  $\mathcal{I} = \mathcal{I}_1 \times \dots \times \mathcal{I}_D$  *partially unbounded* if

$$\exists d \in 1, \dots, D, (\mathcal{I}_d = [a, \infty) \vee \mathcal{I}_d = (-\infty, b])$$

with  $a, b \in \mathbb{R}$ , i.e. when it is either left-bounded by  $-\infty$  or right-bounded by  $\infty$  or unbounded.

## 4 Softmax Saturation on OOD Samples

In this section we will show that, when required to approximate a strictly monotonic function, a neural discriminator exhibits overconfidence in the prediction of a certain class on OOD samples. To this end, we first lay out a necessary assumption and establish some properties of the function to be learned.

**Assumption 1.** Suppose  $p(y|\mathbf{x}) : \mathbb{R}^D \rightarrow [0, 1]^C$  is a component-wise strictly monotonic function on a partially unbounded interval  $\mathcal{I}$  mapping a data sample onto a probability simplex. We assume in the following that a neural discriminator  $p_\theta$  approximating said function will also learn to be component-wise strictly monotonic on  $\mathcal{I}$  up to some approximation error.

For simplicity, we ignore this error in the following derivations.<sup>2</sup> The ability of neural networks to approximate arbitrary functions is well-known and discussed in a plethora of articles; we refer the reader to e.g. [8, 19, 34, 16, 25] for a formal proof. Next we establish that strict monotonicity for  $p_\theta$  entails the same for  $f_\theta$ . For spatial reasons, the proof is moved to Appendix A.2.

**Lemma 1.** If  $p_\theta$  is a component-wise strictly monotonic function on  $\mathcal{I}$ , then so is  $f_\theta$ .

Using this result, we can later show that although logit values of  $f_\theta(\mathbf{x})$  grow when the input is scaled in the limit, this will not be reflected in the softmax probabilities due to the saturating properties of the function.

We proceed to prove two more properties of neural discriminators. In Lemma 2, we establish the saturating property of the softmax, i.e. the model doesn't change its decision anymore in the limit. In Lemma 3 we compare the rate of growth of different components of  $p_\theta$ . Full proofs are given in Appendix sections A.3 and A.4.

**Lemma 2.** Let  $c, c' \in \mathcal{C}$  be two arbitrary classes. It then holds for their corresponding output components (logits) that

$$\lim_{f_\theta(\mathbf{x})_c \rightarrow \pm\infty} \frac{\partial}{\partial f_\theta(\mathbf{x})_{c'}} \bar{\sigma}(f_\theta(\mathbf{x}))_c = 0 \quad (3)$$

**Lemma 3.** Suppose that  $f_\theta$  is a ReLU-network with  $L$  affine transformations. Let  $\alpha \in \mathbb{R}^D$  be a vector s.t.  $\forall d' \neq d, \alpha_{d'} = 1$ . Then it holds for every class  $c \in \mathcal{C}$  and for every  $d \in 1, \dots, D$  that

$$\forall c' \in \mathcal{C}, \lim_{\alpha_d \rightarrow \infty} \left( \frac{\partial}{\partial f_\theta(\mathbf{x})_{c'}} \bar{\sigma}(f_\theta(\mathbf{x}))_c \right)^{-1} \Big|_{\mathbf{x}=\alpha \odot \mathbf{x}'} - \left( \frac{\partial}{\partial x_d} f_\theta(\mathbf{x})_{c'} \right) \Big|_{\mathbf{x}=\alpha \odot \mathbf{x}'} = \infty \quad (4)$$

Finally, we establish in the next lemma the overconfidence of a model given distant, scaled data points. We formulate this property in terms of the  $l_2$ -norm of the gradient  $\nabla_{\mathbf{x}} p_\theta(y = c|\mathbf{x})$ : Generally, in regions of the feature space where the classifier is predicting a high probability score for some class, the probability surface will be flat and small perturbations in the input  $\mathbf{x}$  will not change the prediction. Therefore, the gradient in these regions w.r.t. the input will be flat and short and potentially even correspond to the zero vector, with a norm of (or close to) zero.

**Lemma 4.** [Overconfidence in the limit] Suppose that  $p_\theta$  is a component-wise strictly monotonic function on a partially unbounded  $D$ -interval  $\mathcal{I}$ . Let  $\mathbf{x}' \in \mathbb{R}^D$  be a data sample and  $\alpha \in \mathbb{R}^D$  a vector s.t.  $\forall d' \neq d, \alpha_{d'} = 1$  and  $\alpha \odot \mathbf{x}' \in \mathcal{I}$ . Then it holds that

$$\forall c \in \mathcal{C}, \lim_{\alpha_d \rightarrow \infty} \left\| \nabla_{\mathbf{x}} p_\theta(y = c|\mathbf{x}) \Big|_{\mathbf{x}=\alpha \odot \mathbf{x}'} \right\|_2 = 0$$

*Proof.* We show that one scalar factor contained in the factorization of the gradient  $\nabla_{\mathbf{x}} p_\theta(y = c|\mathbf{x})$  tends to zero the under the given assumptions, having the whole gradient become the zero vector in the limit. We begin by factorizing the gradient  $\nabla_{\mathbf{x}} p_\theta(y = c|\mathbf{x})$  using the multivariate chain rule:

$$\nabla_{\mathbf{x}} p_\theta(y = c|\mathbf{x}) = \sum_{c'=1}^C \frac{\partial}{\partial f_\theta(\mathbf{x})_{c'}} \bar{\sigma}(f_\theta(\mathbf{x}))_c \cdot \nabla_{\mathbf{x}} f_\theta(\mathbf{x})_{c'} \quad (5)$$

<sup>2</sup>However, this will be revisited in the discussion in section 6.

where we have to consider all classes  $c'$  as the softmax score is computed by aggregating all logit values. Then, Lemma 2 implies that the first factor of every part in the sum of Equation 5 will tend to zero in the limit. Lemma 3 ensures that the first factor approximates zero quicker than every component of the gradient  $\nabla_{\mathbf{x}} f_{\boldsymbol{\theta}}(\mathbf{x})_{c'}$  potentially approaching infinity, causing the product to result in the zero vector.<sup>3</sup> As this results in a sum of zero vectors in the limit, this proves the lemma.  $\square$

Under monotonicity assumptions, we have shown that - due to the saturation properties of the softmax - the output probabilities are less and less sensitive to small perturbations of the input in the limit; instead, the model will appear to be very confident in a certain predicted class. This result is used in the next section to prove that this in turn leads to low uncertainty scores for the same input.

## 5 Overconfidence with Uncertainty Estimation Metrics

In Lemma 4, we have established overconfidence in neural discriminators. Common uncertainty estimation metrics are calculated using  $p_{\boldsymbol{\theta}}(y|\mathbf{x})$ , but often employ the more sophisticated methods introduced in Section 3.3. We now proceed to prove that for each of those metrics, the asymptotic behavior is to approach perfect predictive certainty. In all of the following lemmas, we assume that  $p_{\boldsymbol{\theta}}$  is a component-wise strictly monotonic function on a partially unbounded D-interval  $\mathcal{I}$  and that  $\boldsymbol{\alpha} \in \mathbb{R}^D$  is a vector s.t.  $\forall d' \neq d, \alpha_{d'} = 1$ . Further, we assume that for a data sample  $\mathbf{x}' \sim p(\mathbf{x})$  it holds that  $\boldsymbol{\alpha} \odot \mathbf{x}' \in \mathcal{I}$ , i.e. the scaled point is still contained within the interval.

**Lemma 5.** (*Max. softmax probability [18]*) It holds that

$$\lim_{\alpha_d \rightarrow \infty} \left\| \nabla_{\mathbf{x}} \max_{c \in \mathcal{C}} (p_{\boldsymbol{\theta}}(y = c|\mathbf{x})) \Big|_{\mathbf{x} = \boldsymbol{\alpha} \odot \mathbf{x}'} \right\|_2 = 0$$

*Proof.* The gradient of the max function will be a specific  $\nabla_{\mathbf{x}} p_{\boldsymbol{\theta}}(y = c|\mathbf{x})$ , which reduces this to the case already proven in Lemma 4.  $\square$

**Lemma 6.** (*Overconfidence on OOD samples for aggregated predictions*) It holds that

$$\lim_{\alpha_d \rightarrow \infty} \left\| \nabla_{\mathbf{x}} \mathbb{E}_{p(\boldsymbol{\theta}|\mathcal{D})} [p_{\boldsymbol{\theta}}(y = c|\mathbf{x})] \Big|_{\mathbf{x} = \boldsymbol{\alpha} \odot \mathbf{x}'} \right\|_2 = 0$$

The full proofs for this and the following lemmas can be found in appendix sections A.5, A.6, A.7 and A.8. After proving that Lemma 4 also holds in expectation in Lemma 6, the proof strategy for all further metrics is to simplify and reduce the uncertainty metrics such that Lemma 6 can be applied.

**Lemma 7.** (*Asymptotic behavior with softmax variance [22, 24]*) It holds that

$$\lim_{\alpha_d \rightarrow \infty} \left\| \nabla_{\mathbf{x}} \frac{1}{C} \sum_{c=1}^C \mathbb{E}_{p(\boldsymbol{\theta}|\mathcal{D})} \left[ (p_{\boldsymbol{\theta}}(y = c|\mathbf{x}))^2 \right] - \mathbb{E}_{p(\boldsymbol{\theta}|\mathcal{D})} \left[ p_{\boldsymbol{\theta}}(y = c|\mathbf{x}) \right]^2 \Big|_{\mathbf{x} = \boldsymbol{\alpha} \odot \mathbf{x}'} \right\|_2 = 0$$

**Lemma 8.** (*Asymptotic behavior for predictive entropy [11]*) It holds that

$$\lim_{\alpha_d \rightarrow \infty} \left\| \nabla_{\mathbf{x}} \mathbb{H} \left[ \mathbb{E}_{p(\boldsymbol{\theta}|\mathcal{D})} [p_{\boldsymbol{\theta}}(y|\mathbf{x})] \right] \Big|_{\mathbf{x} = \boldsymbol{\alpha} \odot \mathbf{x}'} \right\|_2 = 0$$

**Lemma 9.** (*Asymptotic behavior for approximate mutual information [48]*) It holds that

$$\lim_{\alpha_d \rightarrow \infty} \left\| \nabla_{\mathbf{x}} \left( \mathbb{H} \left[ \mathbb{E}_{p(\boldsymbol{\theta}|\mathcal{D})} [p_{\boldsymbol{\theta}}(y|\mathbf{x})] \right] - \mathbb{E}_{p(\boldsymbol{\theta}|\mathcal{D})} \left[ \mathbb{H} [p_{\boldsymbol{\theta}}(y|\mathbf{x})] \right] \right) \Big|_{\mathbf{x} = \boldsymbol{\alpha} \odot \mathbf{x}'} \right\|_2 = 0$$

All of these result combined now pave the way for our central theorem:

---

<sup>3</sup>Note that the proof of this lemma required proving that the gradient of the expression went to the zero vector in the limit, a fact that will be also used in subsequent proofs.

**Theorem 1** (High certainty in the limit). *Assume that  $p(y|\mathbf{x}) : \mathbb{R}^D \rightarrow [0, 1]^C$  is a component-wise strictly monotonic function on a partially unbounded interval  $\mathcal{I}$ . Suppose a neural network  $p_\theta$  is trained to discriminate between classes on data samples drawn from a distribution  $p(\mathbf{x})$ . Whenever uncertainty is measured via either of the following metrics*

1. *Max. softmax probability*
2. *Softmax variance*
3. *Predictive entropy*
4. *Approximate mutual information*

*the same network(s) will reach perfect certainty as data points in  $\mathcal{I}$  are scaled far away from the training distribution.*

*Proof.* Given assumption 1,  $p_\theta$  will also approximately be a component-wise strictly monotonic function on the partially unbounded interval  $\mathcal{I}$ . The four items of the theorem are then proven separately by lemmas 5, 7, 8 and 9.  $\square$

## 6 Discussion

In the past section, we have proven that - under the assumption that at least one feature enjoys a monotonic relationship with the outcome - a model will become very confident in its predictions on far away samples. The significance of this observation is that, albeit some modest success at OOD detection that might take place locally, the models we analyzed have an inherent overgeneralization bias, ultimately pushing them toward overconfidence on OOD samples. Our results can be seen as a first step to supply a theoretically-motivated explanation to observations such as reported in [48, 43, 1, 26, 51] and to enable the discovery of more effective methods.

The degree to which Assumption 1 is respected, or even just the degree to which  $p_\theta$  is monotonic, can influence OOD detection. For example, on synthetic data in Figure 1 we can see models detecting OOD samples to different extents. Discrepancies among models can be attributed to the distinct approaches in which models approximate the true function  $p(y|\mathbf{x})$ : given that there will be some error in the approximation due to aleatoric and epistemic uncertainty, models may be able to apply the aforementioned uncertainty estimation metrics for OOD detection to some success. For models combining different estimations of the target function, where distinct approximation errors pile up, diversification may contribute to OOD detection in some regions of the feature space. This may however come at the cost of performance (see e.g. discussion in [51]) and anyway have the unwanted consequence that the availability of more in-domain data decreases epistemic uncertainty and diversification, but in so doing worsens OOD detection.

It is worth remarking that the result is relative to an interval  $\mathcal{I}$ . The existence of such interval, and its relevant size compared to the feature space, will vary depending on applications. In practice, it will be sufficient to have a model approximating a function that is monotonic on a single dimension to trigger the undesired behaviour described by the theorem. There are in fact several high-impact applications where such an interval  $\mathcal{I}$  is identifiable, i.e. where there is a clear monotonic relationship between features and classification outcomes. Consider for example the prediction of mortgage default based on past debt: in this binary classification scenario we expect a monotonic relationship between the amount of debt and the risk of default. Another example includes the prediction of cardiovascular complications based on BMI. In all these instances we *want* our models to pick up on those monotonic feature-outcome relationships - models that do not are arguably not desirable - thus it is reasonable to expect that Assumption 1 will be fulfilled to large extent. In all such contexts, the premises of our analysis would be met and the aforementioned methods run a concrete risk of misclassifying OOD samples, with potentially unintended, negative side-effects.

Future research on the topic might be divided on two categories: efforts to solve the problem of OOD detection, and attempts at sharpening our theoretical understanding of the issue. The following approaches fall into the first category: One way could consist of complementing neural discriminators with density-based approaches such as in Grathwohl et al. [14]. Another promising line of research tries to have neural discriminators parametrize Dirichlet instead of categorical distributions [35, 36, 21, 6]. Another very recent approach tries to mitigate the problem discussed by

making models distance-aware [33]. In the second category we can mention that more work is needed to cover the case of categorical features. Reasoning in the limit is not available for discrete categorical variables and one would probably have to resort to techniques that address directly the difference between the training and the new distribution. These investigations, together with reflections on how much the monotonicity assumptions can be relaxed, are left to future work.

## 7 Acknowledgements

We would like to thank Mareike Hartmann, Adam Izdebski, Emese Thamó and Christina Winkler for their tremendously helpful feedback on this work. We would also like to thank Lotta Meijerink for writing the code used to create the illustrations.

## References

- [1] Jonathan Aigrain and Marcin Detyniecki. Detecting adversarial examples and other misclassifications in neural networks by introspection. *arXiv preprint arXiv:1905.09186*, 2019.
- [2] Dario Amodei, Chris Olah, Jacob Steinhardt, Paul Christiano, John Schulman, and Dan Mané. Concrete problems in ai safety. *arXiv preprint arXiv:1606.06565*, 2016.
- [3] Guy Blanc and Steffen Rendle. Adaptive sampled softmax with kernel based sampling. In *International Conference on Machine Learning*, pages 590–599, 2018.
- [4] Charles Blundell, Julien Cornebise, Koray Kavukcuoglu, and Daan Wierstra. Weight uncertainty in neural networks. *arXiv preprint arXiv:1505.05424*, 2015.
- [5] John S Bridle. Probabilistic interpretation of feedforward classification network outputs, with relationships to statistical pattern recognition. In *Neurocomputing*, pages 227–236. Springer, 1990.
- [6] Bertrand Charpentier, Daniel Zügner, and Stephan Günnemann. Posterior network: Uncertainty estimation without ood samples via density-based pseudo-counts. *arXiv preprint arXiv:2006.09239*, 2020.
- [7] Binghui Chen, Weihong Deng, and Junping Du. Noisy softmax: Improving the generalization ability of dcnn via postponing the early softmax saturation. In *Proceedings of the IEEE Conference on Computer Vision and Pattern Recognition*, pages 5372–5381, 2017.
- [8] George Cybenko. Approximation by superpositions of a sigmoidal function. *Mathematics of control, signals and systems*, 2(4):303–314, 1989.
- [9] Alexandre de Brébisson and Pascal Vincent. An exploration of softmax alternatives belonging to the spherical loss family. *arXiv preprint arXiv:1511.05042*, 2015.
- [10] Armen Der Kiureghian and Ove Ditlevsen. Aleatory or epistemic? does it matter? *Structural safety*, 31(2):105–112, 2009.
- [11] Yarin Gal. Uncertainty in deep learning. *University of Cambridge*, 1(3), 2016.
- [12] Yarin Gal and Zoubin Ghahramani. Dropout as a bayesian approximation: Representing model uncertainty in deep learning. In *International conference on Machine Learning*, pages 1050–1059, 2016.
- [13] Bolin Gao and Lacra Pavel. On the properties of the softmax function with application in game theory and reinforcement learning. *arXiv preprint arXiv:1704.00805*, 2017.
- [14] Will Grathwohl, Kuan-Chieh Wang, Jörn-Henrik Jacobsen, David Duvenaud, Mohammad Norouzi, and Kevin Swersky. Your classifier is secretly an energy based model and you should treat it like one. In *8th International Conference on Learning Representations, ICLR 2020, Addis Ababa, Ethiopia, April 26-30, 2020*, 2020.

[15] Chuan Guo, Geoff Pleiss, Yu Sun, and Kilian Q. Weinberger. On calibration of modern neural networks. In *Proceedings of the 34th International Conference on Machine Learning, ICML 2017, Sydney, NSW, Australia, 6-11 August 2017*, pages 1321–1330, 2017.

[16] Boris Hanin. Universal function approximation by deep neural nets with bounded width and relu activations. *Mathematics*, 7(10):992, 2019.

[17] Jianxing He, Sally L Baxter, Jie Xu, Jiming Xu, Xingtao Zhou, and Kang Zhang. The practical implementation of artificial intelligence technologies in medicine. *Nature medicine*, 25(1):30–36, 2019.

[18] Dan Hendrycks and Kevin Gimpel. A baseline for detecting misclassified and out-of-distribution examples in neural networks. In *5th International Conference on Learning Representations, ICLR 2017, Toulon, France, April 24-26, 2017, Conference Track Proceedings*, 2017.

[19] Kurt Hornik. Approximation capabilities of multilayer feedforward networks. *Neural networks*, 4(2):251–257, 1991.

[20] Eyke Hüllermeier and Willem Waegeman. Aleatoric and epistemic uncertainty in machine learning: A tutorial introduction. *arXiv preprint arXiv:1910.09457*, 2019.

[21] Taejong Joo, Uijung Chung, and Min-Gwan Seo. Being bayesian about categorical probability. *CoRR*, abs/2002.07965, 2020.

[22] Michael Kampffmeyer, Arnt-Børre Salberg, and Robert Jenssen. Semantic segmentation of small objects and modeling of uncertainty in urban remote sensing images using deep convolutional neural networks. In *2016 IEEE Conference on Computer Vision and Pattern Recognition Workshops, CVPR Workshops 2016, Las Vegas, NV, USA, June 26 - July 1, 2016*, pages 680–688, 2016.

[23] Sekitoshi Kanai, Yasuhiro Fujiwara, Yuki Yamanaka, and Shuichi Adachi. Sigsoftmax: Re-analysis of the softmax bottleneck. In *Advances in Neural Information Processing Systems 31: Annual Conference on Neural Information Processing Systems 2018, NeurIPS 2018, 3-8 December 2018, Montréal, Canada*, pages 284–294, 2018.

[24] Alex Kendall, Vijay Badrinarayanan, and Roberto Cipolla. Bayesian segnet: Model uncertainty in deep convolutional encoder-decoder architectures for scene understanding. In *British Machine Vision Conference 2017, BMVC 2017, London, UK, September 4-7, 2017*, 2017.

[25] Patrick Kidger and Terry Lyons. Universal approximation with deep narrow networks. In *Conference on Learning Theory*, pages 2306–2327. PMLR, 2020.

[26] Benjamin Kompa, Jasper Snoek, and Andrew Beam. Empirical frequentist coverage of deep learning uncertainty quantification procedures. *arXiv preprint arXiv:2010.03039*, 2020.

[27] Meelis Kull, Miquel Perelló-Nieto, Markus Kängsepp, Telmo de Menezes e Silva Filho, Hao Song, and Peter A. Flach. Beyond temperature scaling: Obtaining well-calibrated multiclass probabilities with dirichlet calibration. *CoRR*, abs/1910.12656, 2019.

[28] Aviral Kumar, Sunita Sarawagi, and Ujjwal Jain. Trainable calibration measures for neural networks from kernel mean embeddings. In *Proceedings of the 35th International Conference on Machine Learning, ICML 2018, Stockholmsmässan, Stockholm, Sweden, July 10-15, 2018*, pages 2810–2819, 2018.

[29] Sachin Kumar and Yulia Tsvetkov. Von mises-fisher loss for training sequence to sequence models with continuous outputs. *CoRR*, abs/1812.04616, 2018.

[30] Anirban Laha, Saneem Ahmed Chemmengath, Priyanka Agrawal, Mitesh Khapra, Karthik Sankaranarayanan, and Harish G Ramaswamy. On controllable sparse alternatives to softmax. In *Advances in Neural Information Processing Systems*, pages 6422–6432, 2018.

[31] Balaji Lakshminarayanan, Alexander Pritzel, and Charles Blundell. Simple and scalable predictive uncertainty estimation using deep ensembles. In *Advances in neural information processing systems*, pages 6402–6413, 2017.

[32] Max-Heinrich Laves, Sontje Ihler, Karl-Philipp Kortmann, and Tobias Ortmaier. Well-calibrated model uncertainty with temperature scaling for dropout variational inference. *4th workshop on Bayesian Deep Learning (NeurIPS 2019), Vancouver, Canada*, 2019.

[33] Jeremiah Liu, Zi Lin, Shreyas Padhy, Dustin Tran, Tania Bedrax Weiss, and Balaji Lakshminarayanan. Simple and principled uncertainty estimation with deterministic deep learning via distance awareness. *Advances in Neural Information Processing Systems*, 33, 2020.

[34] Zhou Lu, Hongming Pu, Feicheng Wang, Zhiqiang Hu, and Liwei Wang. The expressive power of neural networks: A view from the width. In *Advances in neural information processing systems*, pages 6231–6239, 2017.

[35] Andrey Malinin and Mark Gales. Predictive uncertainty estimation via prior networks. In *Advances in Neural Information Processing Systems*, pages 7047–7058, 2018.

[36] Andrey Malinin and Mark J. F. Gales. Reverse kl-divergence training of prior networks: Improved uncertainty and adversarial robustness. In *Advances in Neural Information Processing Systems 32: Annual Conference on Neural Information Processing Systems 2019, NeurIPS 2019, 8-14 December 2019, Vancouver, BC, Canada*, pages 14520–14531, 2019.

[37] Andre Martins and Ramon Astudillo. From softmax to sparsemax: A sparse model of attention and multi-label classification. In *International Conference on Machine Learning*, pages 1614–1623, 2016.

[38] John Alexander McDermid, Yan Jia, and Ibrahim Habli. Towards a framework for safety assurance of autonomous systems. In *Artificial Intelligence Safety 2019*, pages 1–7. CEUR Workshop Proceedings, 2019.

[39] Lotta Meijerink, Giovanni Cinà, and Michele Tonutti. Uncertainty estimation for classification and risk prediction in medical settings. *arXiv preprint arXiv:2004.05824*, 2020.

[40] Jose G Moreno-Torres, Troy Raeder, Rocío Alaiz-Rodríguez, Nitesh V Chawla, and Francisco Herrera. A unifying view on dataset shift in classification. *Pattern recognition*, 45(1):521–530, 2012.

[41] Eric T. Nalisnick, Akihiro Matsukawa, Yee Whye Teh, Dilan Görür, and Balaji Lakshminarayanan. Do deep generative models know what they don’t know? *CoRR*, abs/1810.09136, 2018.

[42] Kirill Neklyudov, Max Welling, Evgenii Egorov, and Dmitry P. Vetrov. Involutive MCMC: a unifying framework. In *Proceedings of the 37th International Conference on Machine Learning, ICML 2020, 13-18 July 2020, Virtual Event*, pages 7273–7282, 2020.

[43] Yaniv Ovadia, Emily Fertig, Jie Ren, Zachary Nado, David Sculley, Sebastian Nowozin, Joshua Dillon, Balaji Lakshminarayanan, and Jasper Snoek. Can you trust your model’s uncertainty? evaluating predictive uncertainty under dataset shift. In *Advances in Neural Information Processing Systems*, pages 13991–14002, 2019.

[44] Tim Pearce, Felix Leibfried, and Alexandra Brintrup. Uncertainty in neural networks: Approximately bayesian ensembling. In *International Conference on Artificial Intelligence and Statistics*, pages 234–244, 2020.

[45] Prajit Ramachandran, Barret Zoph, and Quoc V. Le. Searching for activation functions. *CoRR*, abs/1710.05941, 2017.

[46] Ankit Singh Rawat, Jiecao Chen, Felix Xinnan X Yu, Ananda Theertha Suresh, and Sanjiv Kumar. Sampled softmax with random fourier features. In *Advances in Neural Information Processing Systems*, pages 13857–13867, 2019.

[47] Hidetoshi Shimodaira. Improving predictive inference under covariate shift by weighting the log-likelihood function. *Journal of statistical planning and inference*, 90(2):227–244, 2000.

[48] Lewis Smith and Yarin Gal. Understanding measures of uncertainty for adversarial example detection. In *Proceedings of the Thirty-Fourth Conference on Uncertainty in Artificial Intelligence, UAI 2018, Monterey, California, USA, August 6-10, 2018*, pages 560–569, 2018.

[49] Rohan Taori, Achal Dave, Vaishaal Shankar, Nicholas Carlini, Benjamin Recht, and Ludwig Schmidt. Measuring robustness to natural distribution shifts in image classification. *Advances in Neural Information Processing Systems*, 33, 2020.

[50] Sunil Thulasidasan, Gopinath Chennupati, Jeff A. Bilmes, Tanmoy Bhattacharya, and Sarah Michalak. On mixup training: Improved calibration and predictive uncertainty for deep neural networks. In *Advances in Neural Information Processing Systems 32: Annual Conference on Neural Information Processing Systems 2019, NeurIPS 2019, 8-14 December 2019, Vancouver, BC, Canada*, pages 13888–13899, 2019.

[51] Dennis Ulmer, Lotta Meijerink, and Giovanni Cinà. Trust issues: Uncertainty estimation does not enable reliable ood detection on medical tabular data, 2020.

[52] Max Welling and Yee W Teh. Bayesian learning via stochastic gradient langevin dynamics. In *Proceedings of the 28th international conference on machine learning (ICML-11)*, pages 681–688, 2011.

[53] Zhilin Yang, Zihang Dai, Ruslan Salakhutdinov, and William W. Cohen. Breaking the softmax bottleneck: A high-rank RNN language model. In *6th International Conference on Learning Representations, ICLR 2018, Vancouver, BC, Canada, April 30 - May 3, 2018, Conference Track Proceedings*, 2018.

## A Additional Proofs

This appendix section contains additional proofs and derivations that could not be included in the main paper due to spatial constraints.

### A.1 Connection between Softmax and Sigmoid

In this section we briefly outline the connection between the softmax and the sigmoid function, which was originally shown in [5]. Let the sigmoid function be defined as

$$\sigma(x) = \frac{\exp(x)}{1 + \exp(x)}$$

and softmax according to Equation 1. The output of  $f_{\theta}$  in a multi-class classification problem with  $C$  classes corresponds to a  $C$ -dimensional column vector that is based on an affine transformation of the network’s last intermediate hidden representation  $\mathbf{x}_L$ , such that  $f_{\theta}(\mathbf{x}) = \mathbf{W}_L \mathbf{x}_L$ .<sup>4</sup> Correspondingly, the output of  $f_{\theta}$  for a single class  $c$  can be written as the dot product between  $\mathbf{x}_L$  and the corresponding row vector of  $\mathbf{W}_L$  denoted as  $\mathbf{w}_L^{(c)}$ , such that  $f_{\theta}(\mathbf{x})_c \equiv \mathbf{w}_L^{(c)T} \mathbf{x}_L$ . For a classification problem with  $C = 2$  classes, we can now rewrite the softmax probabilities in the following way:<sup>5</sup>

$$p_{\theta}(y = 1 | \mathbf{x}) = \frac{\exp(\mathbf{w}_L^{(1)T} \mathbf{x}_L)}{\exp(\mathbf{w}_L^{(0)T} \mathbf{x}_L) + \exp(\mathbf{w}_L^{(1)T} \mathbf{x}_L)}$$

Subtracting a constant from the weight term inside the exponential function does not change the output of the softmax function. Using this property, we can show the sigmoid function to be a special case of the softmax for binary classification:

$$\begin{aligned} p_{\theta}(y = 1 | \mathbf{x}) &= \frac{\exp((\mathbf{w}_L^{(1)} - \mathbf{w}_L^{(0)})^T \mathbf{x}_L)}{\exp((\mathbf{w}_L^{(0)} - \mathbf{w}_L^{(0)})^T \mathbf{x}_L) + \exp((\mathbf{w}_L^{(1)} - \mathbf{w}_L^{(0)})^T \mathbf{x}_L)} \\ &= \frac{\exp((\mathbf{w}_L^{(1)} - \mathbf{w}_L^{(0)})^T \mathbf{x}_L)}{1 + \exp((\mathbf{w}_L^{(1)} - \mathbf{w}_L^{(0)})^T \mathbf{x}_L)} = \frac{\exp(\mathbf{w}_L^{*T} \mathbf{x}_L)}{1 + \exp(\mathbf{w}_L^{*T} \mathbf{x}_L)} \end{aligned}$$

where  $\mathbf{w}_L^* = \mathbf{w}_L^{(1)} - \mathbf{w}_L^{(0)}$  corresponds to the new parameter vector which is used to parameterize a single output unit for a network in the binary classification setting.

<sup>4</sup>The bias term  $\mathbf{b}_L$  was omitted here for clarity.

<sup>5</sup>The following argument holds without loss of generality for  $p_{\theta}(y = 0 | \mathbf{x})$

## A.2 Proof of Lemma 1

*Proof.* Let  $d$  be a dimension and  $c$  a component of  $p_{\theta}$ . By assumption, for all points in  $\mathcal{I}$ ,  $p_{\theta}(y|\mathbf{x})_c$ , has either a positive or always negative gradient on this dimension. Suppose the first case. Let  $\mathbf{x}' \in \mathcal{I}$  and  $\gamma \in \mathbb{R}^D$  be a vector s.t.  $\gamma_d > 0$ ,  $\forall d' \neq d$ ,  $\gamma_{d'} = 0$  and  $\mathbf{x}' + \gamma \in \mathcal{I}$ . Since  $\mathbf{x}'_d < \mathbf{x}'_d + \gamma_d$  and the gradient is positive with respect to that dimension, we know by the decomposition of  $p_{\theta} = \bar{\sigma} \circ f_{\theta}$  that  $\bar{\sigma}(f_{\theta}(\mathbf{x}' + \gamma))_c > \bar{\sigma}(f_{\theta}(\mathbf{x}'))_c$ . Since the softmax function is strictly increasing for every component  $c$ , we can conclude that  $f_{\theta}(\mathbf{x}' + \gamma)_c > f_{\theta}(\mathbf{x}')_c$ . It follows that

$$\begin{aligned} f_{\theta}(\mathbf{x}' + \gamma)_c &> f_{\theta}(\mathbf{x}')_c \\ \iff f_{\theta}(\mathbf{x}' + \gamma)_c - f_{\theta}(\mathbf{x}')_c &> 0 \\ \iff \frac{f_{\theta}(\mathbf{x}' + \gamma)_c - f_{\theta}(\mathbf{x}')_c}{\gamma_d} &> 0 \end{aligned}$$

Therefore, the gradient of  $(f_{\theta})_c$  remains positive:

$$\lim_{\gamma_d \rightarrow 0} \frac{f_{\theta}(\mathbf{x}' + \gamma)_c - f_{\theta}(\mathbf{x}')_c}{\gamma_d} = \left( \nabla_{\mathbf{x}} f_{\theta}(\mathbf{x})_c \Big|_{\mathbf{x}=\mathbf{x}'} \right)_d > 0$$

A symmetrical argument shows that if the gradient of  $p_{\theta}(y|\mathbf{x})_c$  is negative in this dimension then so it the gradient of  $f_{\theta}(\mathbf{x})_c$ . Since  $d$  and  $c$  where arbitrary, this holds for all dimensions and all  $c \in \mathcal{C}$ , so  $f_{\theta}$  is a component-wise strictly monotonic function.  $\square$

## A.3 Proof of Lemma 3

*Proof.* We first evaluate the left-hand side of Inequality 4 to show that it grows exponentially in the limit. Given Lemma 2 describing the asymptotic behavior in the limit, it follows naturally that

$$\lim_{f_{\theta}(\mathbf{x})_c \rightarrow \pm\infty} \left( \frac{\partial}{\partial f_{\theta}(\mathbf{x})_c} \bar{\sigma}(f_{\theta}(\mathbf{x}))_c \right)^{-1} = \infty$$

where we can see that the result is a symmetrical function displaying exponential growth in the limit of  $f_{\theta}(\mathbf{x})_c \rightarrow \pm\infty$ . Now note that because we assumed  $f_{\theta}$  to be a neural network consisting of  $L$  affine transformations with ReLU activation functions, the output of each layer is only going to be a linear combination of its inputs.<sup>6</sup> This can be proven by induction. Let us first look at the base case  $L = 1$ . In the rest of this proof, we denote  $\mathbf{x}_l$  as the input to layer  $l$ , with  $\mathbf{x}_0 \equiv \mathbf{x}$ , and  $\mathbf{W}_l, \mathbf{b}_l$  the corresponding layer parameters.  $\mathbf{a}_l$  signifies the result of the affine transformation that is then fed into the activation function.

$$\begin{aligned} f_{\theta}(\mathbf{x}) &= \text{ReLU}(\mathbf{a}_0) = \text{ReLU}(\mathbf{W}_0 \mathbf{x}_0 + \mathbf{b}_0) \\ \frac{\partial f_{\theta}(\mathbf{x})}{\partial \mathbf{x}_0} &= \frac{\text{ReLU}(\mathbf{a}_0)}{\partial \mathbf{a}_0} \frac{\partial \mathbf{a}_0}{\partial \mathbf{x}_0} = \mathbb{1}(\mathbf{x}_0)^T \mathbf{W}_0 \\ \frac{\partial f_{\theta}(\mathbf{x})}{\partial \mathbf{x}_{0d}} &= \mathbb{1}(x_d > 0) \mathbf{W}_{0d} \end{aligned} \tag{6}$$

where  $\mathbb{1}(\mathbf{x}_0) = [\mathbb{1}(x_{01} > 0), \dots, \mathbb{1}(x_{0D} > 0)]^T$  and  $\mathbf{W}_{0d}$  denotes the  $d$ -th column of  $\mathbf{W}_0$ . This is a linear function, which proves the base case. Let now  $\frac{\partial \mathbf{x}_{l+1}}{\partial \mathbf{x}_l}$  denote the partial derivative of the input to the  $l$ -th layer w.r.t to the input and suppose that it is linear by the inductive hypothesis. Augmenting the corresponding network by another linear adds another term akin to the second expression in Equation 6

$$\frac{\partial \mathbf{x}_{l+1}}{\partial \mathbf{x}_l} \frac{\partial \mathbf{x}_l}{\partial \mathbf{x}_0} = \frac{\partial \mathbf{x}_{l+1}}{\partial \mathbf{x}_0} \tag{7}$$

which is also a linear function of  $\mathbf{x}_{l+1}$ , proving the induction step. Because we know that both terms of the product in Equation 7 are linear, the right-hand side of Inequality 4 is as well. Together with the previous insight that the left-hand side is exponential, this proves the lemma.  $\square$

<sup>6</sup>We here make the argument for the whole function  $f_{\theta} : \mathbb{R}^D \rightarrow \mathbb{R}^C$ , but the conclusions also applies to every output component of the function  $f_{\theta}(\mathbf{x})_c$  which is mentioned in 4.

#### A.4 Proof of Lemma 2

*Proof.* Here, we first begin by evaluating the derivative of one component of the function w.r.t to an arbitrary component:

$$\begin{aligned} \frac{\partial}{\partial f_{\theta}(\mathbf{x})_{c'}} \bar{\sigma}(f_{\theta}(\mathbf{x}))_c &= \frac{\partial}{\partial f_{\theta}(\mathbf{x})_{c'}} \frac{\exp(f_{\theta}(\mathbf{x})_c)}{\sum_{c'' \in \mathcal{C}} \exp(f_{\theta}(\mathbf{x})_{c''})} \\ &= \frac{\mathbb{1}(c = c') \exp(f_{\theta}(\mathbf{x})_c)}{\sum_{c'' \in \mathcal{C}} \exp(f_{\theta}(\mathbf{x})_{c''})} - \frac{\exp(f_{\theta}(\mathbf{x})_c) \exp(f_{\theta}(\mathbf{x})_{c'})}{\left(\sum_{c'' \in \mathcal{C}} \exp(f_{\theta}(\mathbf{x})_{c''})\right)^2} \end{aligned}$$

This implies that

$$\frac{\partial}{\partial f_{\theta}(\mathbf{x})_{c'}} \bar{\sigma}(f_{\theta}(\mathbf{x}))_c = \begin{cases} -\frac{\exp(2f_{\theta}(\mathbf{x})_c)}{\left(\sum_{c'' \in \mathcal{C}} \exp(f_{\theta}(\mathbf{x})_{c''})\right)^2} + \frac{\exp(f_{\theta}(\mathbf{x})_c)}{\sum_{c'' \in \mathcal{C}} \exp(f_{\theta}(\mathbf{x})_{c''})} & \text{If } c = c' \\ -\frac{\exp(f_{\theta}(\mathbf{x})_c + f_{\theta}(\mathbf{x})_{c'})}{\left(\sum_{c'' \in \mathcal{C}} \exp(f_{\theta}(\mathbf{x})_{c''})\right)^2} & \text{If } c \neq c' \end{cases} \quad (8)$$

or more compactly:

$$\frac{\partial}{\partial f_{\theta}(\mathbf{x})_{c'}} \bar{\sigma}(f_{\theta}(\mathbf{x}))_c = \bar{\sigma}(f_{\theta}(\mathbf{x}))_c (\mathbb{1}(c = c') - \bar{\sigma}(f_{\theta}(\mathbf{x}))_{c'})$$

Based on Equation 8, we can now investigate the asymptotic behavior for  $f_{\theta}(\mathbf{x})_c \rightarrow \infty$  more easily, starting with the  $c = c'$  case:

$$\begin{aligned} \lim_{f_{\theta}(\mathbf{x})_c \rightarrow \infty} \frac{\partial}{\partial f_{\theta}(\mathbf{x})_{c'}} \bar{\sigma}(f_{\theta}(\mathbf{x}))_c &= \underbrace{\lim_{f_{\theta}(\mathbf{x})_c \rightarrow \infty} -\frac{\exp(f_{\theta}(\mathbf{x})_c)}{\sum_{c'' \in \mathcal{C}} \exp(f_{\theta}(\mathbf{x})_{c''})} \frac{\exp(f_{\theta}(\mathbf{x})_c)}{\sum_{c'' \in \mathcal{C}} \exp(f_{\theta}(\mathbf{x})_{c''})}}_{-1} \\ &\quad + \underbrace{\lim_{f_{\theta}(\mathbf{x})_c \rightarrow \infty} \frac{\exp(f_{\theta}(\mathbf{x})_c)}{\sum_{c'' \in \mathcal{C}} \exp(f_{\theta}(\mathbf{x})_{c''})}}_1 = 0 \end{aligned} \quad (9)$$

With the numerator and denominator being dominated by the exponentiated  $f_{\theta}(\mathbf{x})_c$  in Equation 9, the first term will tend to  $-1$ , while the second term will tend to  $1$ , resulting in a derivative of  $0$ . The  $c \neq c'$  can be analyzed the following way:

$$\begin{aligned} \lim_{f_{\theta}(\mathbf{x})_c \rightarrow \infty} \frac{\partial}{\partial f_{\theta}(\mathbf{x})_{c'}} \bar{\sigma}(f_{\theta}(\mathbf{x}))_c &= \underbrace{\lim_{f_{\theta}(\mathbf{x})_c \rightarrow \infty} \left( -\frac{\exp(f_{\theta}(\mathbf{x})_c)}{\sum_{c'' \in \mathcal{C}} \exp(f_{\theta}(\mathbf{x})_{c''})} \right)}_{-1} \\ &\quad \cdot \underbrace{\lim_{f_{\theta}(\mathbf{x})_c \rightarrow \infty} \left( \frac{\exp(f_{\theta}(\mathbf{x})_{c'})}{\sum_{c'' \in \mathcal{C}} \exp(f_{\theta}(\mathbf{x})_{c''})} \right)}_0 = 0 \end{aligned} \quad (10)$$

Again, we factorize the fraction in Equation 10 into the product of two softmax functions, one for component  $c$ , one for  $c'$ . The first factor will again tend to  $-1$  as in the other case, however the second will approach  $0$ , as only the sum in the denominator will approach infinity. As the limit of a product is the products of its limits, this lets the whole expression approach  $0$  in the limit.

When  $f_{\theta}(\mathbf{x})_c \rightarrow -\infty$ , both cases approach  $0$  due to the exponential function, which proves the lemma.  $\square$

How to interplay between different softmax components produces zero gradients in the limit is illustrated in Figure 2.

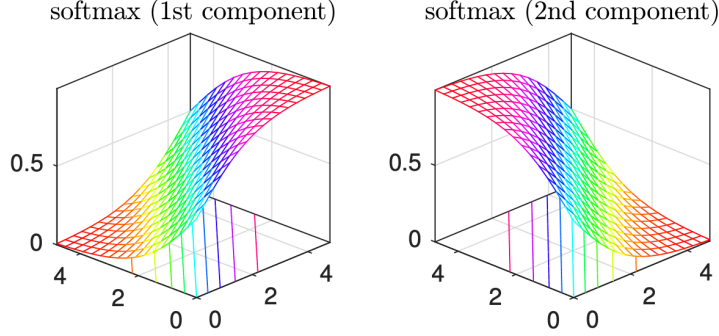


Figure 2: Illustration taken from the work of [13], illustrating the interplay of softmax probabilities between components for  $C = 2$  in  $\mathbb{R}^2$ .

### A.5 Proof of Lemma 6

*Proof.*

$$\lim_{\alpha \rightarrow \infty} \left\| \nabla_{\mathbf{x}} \mathbb{E}_{p(\boldsymbol{\theta} | \mathcal{D})} \left[ p_{\boldsymbol{\theta}}(y = c | \mathbf{x}) \right] \right\|_{\mathbf{x} = \boldsymbol{\alpha} \odot \mathbf{x}'}_2$$

Linearity of gradient:

$$= \lim_{\alpha \rightarrow \infty} \left\| \mathbb{E}_{p(\boldsymbol{\theta} | \mathcal{D})} \left[ \nabla_{\mathbf{x}} p_{\boldsymbol{\theta}}(y = c | \mathbf{x}) \right] \right\|_{\mathbf{x} = \boldsymbol{\alpha} \odot \mathbf{x}'}_2$$

Utilize Jensen's inequality  $\phi(\mathbb{E}[\mathbf{x}]) \leq \mathbb{E}[\phi(\mathbf{x})]$  as  $l_2$ -norm is a convex function and Lemma 4:

$$\leq \lim_{\alpha \rightarrow \infty} \mathbb{E}_{p(\boldsymbol{\theta} | \mathcal{D})} \left[ \underbrace{\left\| \nabla_{\mathbf{x}} p_{\boldsymbol{\theta}}(y = c | \mathbf{x}) \right\|_{\mathbf{x} = \boldsymbol{\alpha} \odot \mathbf{x}'}_2}_{{}=0 \text{ (Lemma 4)}} \right] = 0$$

Because the last expression is an upper bound to the original expression and the  $l_2$  norm is lower-bounded by 0, this proves the lemma.  $\square$

### A.6 Proof of Lemma 7

*Proof.*

$$\lim_{\alpha \rightarrow \infty} \left\| \nabla_{\mathbf{x}} \frac{1}{C} \sum_{c=1}^C \mathbb{E}_{p(\boldsymbol{\theta} | \mathcal{D})} \left[ \left( p_{\boldsymbol{\theta}}(y = c | \mathbf{x}) \right)^2 \right] - \mathbb{E}_{p(\boldsymbol{\theta} | \mathcal{D})} \left[ p_{\boldsymbol{\theta}}(y = c | \mathbf{x}) \right]^2 \right\|_{\mathbf{x} = \boldsymbol{\alpha} \odot \mathbf{x}'}_2$$

Linearity of gradient:

$$= \lim_{\alpha_d \rightarrow \infty} \left\| \frac{1}{C} \sum_{c=1}^C \nabla_{\mathbf{x}} \mathbb{E}_{p(\boldsymbol{\theta} | \mathcal{D})} \left[ \left( p_{\boldsymbol{\theta}}(y = c | \mathbf{x}) \right)^2 \right] - \nabla_{\mathbf{x}} \mathbb{E}_{p(\boldsymbol{\theta} | \mathcal{D})} \left[ p_{\boldsymbol{\theta}}(y = c | \mathbf{x}) \right]^2 \right\|_{\mathbf{x} = \boldsymbol{\alpha} \odot \mathbf{x}'}_2$$

Apply triangle inequality  $\|x + y\| \leq \|x\| + \|y\|$  to sum over all  $c$ :

$$\leq \lim_{\alpha_d \rightarrow \infty} \frac{1}{C} \sum_{c=1}^C \left\| \nabla_{\mathbf{x}} \mathbb{E}_{p(\boldsymbol{\theta} | \mathcal{D})} \left[ \left( p_{\boldsymbol{\theta}}(y = c | \mathbf{x}) \right)^2 \right] - \nabla_{\mathbf{x}} \mathbb{E}_{p(\boldsymbol{\theta} | \mathcal{D})} \left[ p_{\boldsymbol{\theta}}(y = c | \mathbf{x}) \right]^2 \right\|_{\mathbf{x} = \boldsymbol{\alpha} \odot \mathbf{x}'}_2$$

On the first term use linearity of gradients and apply chain rule, do it in the reverse order on the second term:

$$\begin{aligned}
&= \lim_{\alpha_d \rightarrow \infty} \frac{1}{C} \sum_{c=1}^C \left\| \mathbb{E}_{p(\theta|\mathcal{D})} \left[ 2p_{\theta}(y=c|\mathbf{x}) \nabla_{\mathbf{x}} p_{\theta}(y=c|\mathbf{x}) \right] \Big|_{\mathbf{x}=\alpha \odot \mathbf{x}'} \right. \\
&\quad \left. \underbrace{\quad}_{=0 \text{ (Lemma 4)}} \right. \\
&\quad - \left( 2\mathbb{E}_{p(\theta|\mathcal{D})} \left[ p_{\theta}(y=c|\mathbf{x}) \right] \right) \mathbb{E}_{p(\theta|\mathcal{D})} \left[ \underbrace{\nabla_{\mathbf{x}} p_{\theta}(y=c|\mathbf{x})}_{=0 \text{ (Lemma 4)}} \Big|_{\mathbf{x}=\alpha \odot \mathbf{x}'} \right] \Big\|_2 = 0
\end{aligned}$$

We can see that due to an intermediate result of Lemma 4, i.e. that  $\nabla_{\mathbf{x}} p_{\theta}(y=c|\mathbf{x})$  approaches the zero vector in the limit, the innermost gradients tend to zero, bringing the whole expression to 0.

Because the final is an upper bound to the original expression and because the  $l_2$  norm has a lower bound of 0, this proves the lemma.  $\square$

## A.7 Proof of Lemma 8

*Proof.*

$$\begin{aligned}
&\lim_{\alpha_d \rightarrow \infty} \left\| \nabla_{\mathbf{x}} \mathbb{H} \left[ \mathbb{E}_{p(\theta|\mathcal{D})} \left[ p_{\theta}(y|\mathbf{x}) \right] \right] \Big|_{\mathbf{x}=\alpha \odot \mathbf{x}'} \right\|_2 \\
&= \lim_{\alpha_d \rightarrow \infty} \left\| \nabla_{\mathbf{x}} \left( \sum_{c=1}^C \mathbb{E}_{p(\theta|\mathcal{D})} \left[ p_{\theta}(y=c|\mathbf{x}) \right] \log \left( \mathbb{E}_{p(\theta|\mathcal{D})} \left[ p_{\theta}(y=c|\mathbf{x}) \right] \right) \right) \Big|_{\mathbf{x}=\alpha \odot \mathbf{x}'} \right\|_2
\end{aligned}$$

Linearity of gradient:

$$= \lim_{\alpha_d \rightarrow \infty} \left\| \sum_{c=1}^C \nabla_{\mathbf{x}} \left( \mathbb{E}_{p(\theta|\mathcal{D})} \left[ p_{\theta}(y=c|\mathbf{x}) \right] \log \left( \mathbb{E}_{p(\theta|\mathcal{D})} \left[ p_{\theta}(y=c|\mathbf{x}) \right] \right) \right) \Big|_{\mathbf{x}=\alpha \odot \mathbf{x}'} \right\|_2$$

Apply product rule:

$$\begin{aligned}
&= \lim_{\alpha_d \rightarrow \infty} \left\| \left( \sum_{c=1}^C \underbrace{\mathbb{E}_{p(\theta|\mathcal{D})} \left[ p_{\theta}(y=c|\mathbf{x}) \right]}_{=1} \cdot \left( \mathbb{E}_{p(\theta|\mathcal{D})} \left[ p_{\theta}(y=c|\mathbf{x}) \right] \right)^{-1} \cdot \nabla_{\mathbf{x}} \left( \mathbb{E}_{p(\theta|\mathcal{D})} \left[ p_{\theta}(y=c|\mathbf{x}) \right] \right) \right. \right. \\
&\quad \left. \left. + \nabla_{\mathbf{x}} \left( \mathbb{E}_{p(\theta|\mathcal{D})} \left[ p_{\theta}(y=c|\mathbf{x}) \right] \right) \log \left( \mathbb{E}_{p(\theta|\mathcal{D})} \left[ p_{\theta}(y=c|\mathbf{x}) \right] \right) \right) \Big|_{\mathbf{x}=\alpha \odot \mathbf{x}'} \right\|_2
\end{aligned}$$

Factor out gradient:

$$= \lim_{\alpha_d \rightarrow \infty} \left\| \sum_{c=1}^C \nabla_{\mathbf{x}} \mathbb{E}_{p(\theta|\mathcal{D})} \left[ p_{\theta}(y=c|\mathbf{x}) \right] \left( 1 + \log \left( \mathbb{E}_{p(\theta|\mathcal{D})} \left[ p_{\theta}(y=c|\mathbf{x}) \right] \right) \right) \Big|_{\mathbf{x}=\alpha \odot \mathbf{x}'} \right\|_2$$

Apply triangle inequality to sum over all  $c$ :

$$\leq \lim_{\alpha_d \rightarrow \infty} \sum_{c=1}^C \left\| \nabla_{\mathbf{x}} \mathbb{E}_{p(\theta|\mathcal{D})} \left[ p_{\theta}(y=c|\mathbf{x}) \right] \left( 1 + \log \left( \mathbb{E}_{p(\theta|\mathcal{D})} \left[ p_{\theta}(y=c|\mathbf{x}) \right] \right) \right) \Big|_{\mathbf{x}=\alpha \odot \mathbf{x}'} \right\|_2$$

As the log expectation just evaluates to a scalar, it can be pulled out of the norm and we can apply Lemma 6

$$= \lim_{\alpha_d \rightarrow \infty} \sum_{c=1}^C \underbrace{\left( 1 + \log \left( \mathbb{E}_{p(\theta|\mathcal{D})} [p_\theta(y=c|\mathbf{x})] \right) \right)}_{\text{Scalar}} \cdot \underbrace{\left\| \nabla_{\mathbf{x}} \mathbb{E}_{p(\theta|\mathcal{D})} [p_\theta(y=c|\mathbf{x})] \right\|_{\mathbf{x}=\alpha \odot \mathbf{x}'}_2}_{=0 \text{ (Lemma 6)}} = 0$$

As the final result is an upper bound to the original expression and is lower-bounded by 0 due to the  $l_2$  norm, this proves the lemma.  $\square$

### A.8 Proof of Lemma 9

*Proof.*

$$\lim_{\alpha_d \rightarrow \infty} \left\| \nabla_{\mathbf{x}} \left( \mathbb{H} \left[ \mathbb{E}_{p(\theta|\mathcal{D})} [p_\theta(y|\mathbf{x})] \right] - \mathbb{E}_{p(\theta|\mathcal{D})} \left[ \mathbb{H} [p_\theta(y|\mathbf{x})] \right] \right) \right\|_{\mathbf{x}=\alpha \odot \mathbf{x}'}$$

Linearity of gradients:

$$\leq \lim_{\alpha_d \rightarrow \infty} \left\| \left( \nabla_{\mathbf{x}} \mathbb{H} \left[ \mathbb{E}_{p(\theta|\mathcal{D})} [p_\theta(y|\mathbf{x})] \right] - \nabla_{\mathbf{x}} \mathbb{E}_{p(\theta|\mathcal{D})} \left[ \mathbb{H} [p_\theta(y|\mathbf{x})] \right] \right) \right\|_{\mathbf{x}=\alpha \odot \mathbf{x}'}$$

Linearity of gradients on second part of difference:

$$= \lim_{\alpha_d \rightarrow \infty} \left\| \left( \nabla_{\mathbf{x}} \mathbb{H} \left[ \mathbb{E}_{p(\theta|\mathcal{D})} [p_\theta(y|\mathbf{x})] \right] - \mathbb{E}_{p(\theta|\mathcal{D})} \left[ \nabla_{\mathbf{x}} \mathbb{H} [p_\theta(y|\mathbf{x})] \right] \right) \right\|_{\mathbf{x}=\alpha \odot \mathbf{x}'}$$

Applying chain rule and intermediate result of Lemma 4:

$$\begin{aligned} &= \lim_{\alpha_d \rightarrow \infty} \left\| \nabla_{\mathbf{x}} \mathbb{H} \left[ \mathbb{E}_{p(\theta|\mathcal{D})} [p_\theta(y|\mathbf{x})] \right] \right\|_{\mathbf{x}=\alpha \odot \mathbf{x}'} \\ &\quad - \mathbb{E}_{p(\theta|\mathcal{D})} \left[ \sum_{c=1}^C \left( 1 + \log p_\theta(y=c|\mathbf{x}) \right) \underbrace{\nabla_{\mathbf{x}} p_\theta(y=c|\mathbf{x})}_{=0 \text{ (Lemma 4)}} \right] \right\|_{\mathbf{x}=\alpha \odot \mathbf{x}'}_2 \end{aligned}$$

Because this lets the entire second term become the zero vector in the limit, the remaining part reduces to the case proven in Lemma 8:

$$= \underbrace{\lim_{\alpha_d \rightarrow \infty} \left\| \nabla_{\mathbf{x}} \mathbb{H} \left[ \mathbb{E}_{p(\theta|\mathcal{D})} [p_\theta(y|\mathbf{x})] \right] \right\|_{\mathbf{x}=\alpha \odot \mathbf{x}'}}_{\text{Lemma 8}}_2 = 0$$

As the final result is an upper bound to the original expression and the  $l_2$  norm provides a lower bound of 0, this proves the lemma.  $\square$